Reactive Compatibilization of SAN/EPR Blends. 1. Dependence of the Phase Morphology Development on the Reaction Kinetics

Christophe Pagnoulle,[†] Cor Koning,[‡] Luc Leemans,[‡] and Robert Jérôme*[,†]

Center for Education and Research on Macromolecules (CERM), University of Liège, Sart-Tilman, B6, 4000 Liège, Belgium, and DSM Research, P.O. Box 18, 6160 MD, Geleen, The Netherlands

Received August 5, 1999; Revised Manuscript Received June 5, 2000

ABSTRACT: SAN containing 20 wt % of reactive SAN-X has been melt blended with EPDM containing 50 wt % of EP chains grafted by maleic anhydride (EP-*g*-MA). Two types of reactive groups (X) have been attached to SAN (2 mol % of X), i.e., a primary amine and a precursor of it at the processing temperature, i.e., a carbamate. The SAN/rubber weight composition was kept constant at 75/25. The development of the phase morphology from pellet-sized rubber particles to dispersed submicrometer droplets has been investigated during reactive mixing for the two types of reactive SAN and has been found to depend on the interpolymer reaction rate and thus on the relative reactivity of the amine and the carbamate groups attached to SAN toward the maleic anhydride function of EP.

1. Introduction

Since most polymers are immiscible, polyblends have usually to be compatibilized in order to improve poor mechanical performances associated with a gross phase morphology and a low interfacial adhesion. Efficiency of block and graft copolymers in reducing the interfacial tension and improving the interfacial adhesion has been extensively discussed elsewhere.[1,2] These additives can be premade or generated in situ in a reactive blending process. Reactive blending has the advantage to be straightforward and to form the compatibilizer where it has to be localized, i.e., at the interface.

One of the key factors to provide polyblends with the desired mechanical properties is the control of their phase morphology. How the blend morphology is developed during the early stage of the melt blending, i.e., from pellet or powder sized particles to final submicron phases, is of prime importance. Indeed, Scott and Sundararaj have shown that the major reduction of the particle size of reactive blends, i.e., polyamide/polystyrene and polypropylene/polystyrene, in a batch mixer or in a twin-screw extruder, occurred during the softening/melting step of the blend components.[3,4] Consistently, in the case of highly PP/PC immiscible blends, Favis has not observed significant reduction in the size of the dispersed phase beyond 2 min mixing.[5] Similar conclusion has been drawn by De Roover[6] in the reactive blending of a nylon and PP grafted by maleic anhydride. However, in contrast to these observations, Bourry and Favis have recently reported that the final phase morphology of PS/HDPE blends was independent of the melting or the softening step but predominantly settled down in the melt state.[7]

In reactive blending, kinetics and completeness of interfacial reaction with respect to the blending time may be anticipated to control the compatibilization reaction, i.e., the phase morphology and the mechanical properties of the final polyblends. Indeed, the amount and molecular architecture of the copolymer formed at the interface have to be kinetically controlled, which addresses the issue of the intrinsic reactivity of the functional groups attached to the chains that have to react at the interface. In this respect, Scott et al. have compared reactive blending on the basis of the reaction of maleic anhydride (MA) with amine and oxazoline (OX).[8] Unfortunately, the comparison is not straightforward since different polymer pairs have been studied, i.e., EP-MA/PS-OX and PS-MA/PA-NH_2, respectively. Under these experimental conditions, the changes in the mixing torque and the average particle size have been observed to be delayed in time and less pronounced in the case of the MA/OX reactive pair compared to the MA/NH_2 one, consistent with the lower reactivity of the former pair.[8] In a very interesting paper, Orr et al. have compared the reaction rates of aliphatic amine and aromatic amine end-functionalized PS toward anhydride terminal PI at 180 °C.[9] The reaction of the aliphatic amine appeared to be much faster compared to the aromatic one and results in a molecular scale self-assembly into cylinder micelles within 2 min mixing. In contrast, in the case of the slower reactive aromatic amine, the blend did not achieve molecular scale morphology or higher conversion even after 90 min mixing.

Scheme 1. Equation of Carbamate Thermal Decomposition

$$\text{SAN-NH-C(O)-O-C-(CH}_3)_3 \rightarrow \text{SAN-NH}_2 + \text{CO}_2\uparrow + \text{CH}_2\text{=C-(CH}_3)_2\uparrow$$

In this study, maleic anhydride attached to EP chains will be reacted in the melt with either carbamate or amine groups grafted onto SAN chains. In the case of SAN bearing carbamate groups, the interfacial reaction is controlled by the (slow) carbamate thermolysis into primary amine (Scheme 1). Indeed, compared to SAN−NH_2, the grafting of SAN−carbamate has been shown to proceed more slowly at 200 °C under static conditions.[10] This system is ideal to address the question of the mutual reactivity of the functional groups while keeping constant the molecular weight of each polymer (EP and SAN) and the content and distribution of each type of reactive groups in the reactive chains. This system will be studied with the purpose of compatibilizing SAN/EPDM blends.

[†] University of Liège.
[‡] DSM Research.
* To whom correspondence should be addressed.

10.1021/ma991314d CCC: $19.00
Published on Web 08/02/2000

Scheme 2. [1-Methyl-1-[3-(1-methylethenyl)-phenyl]ethyl}Carbamic Acid 1,1-Dimethylethyl Ester

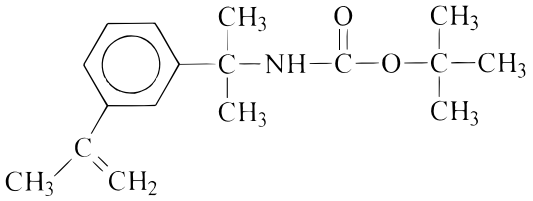

In this work, reactive SAN−X, where X is either a carbamate or a primary amine (0.028 mol X/wt %, i.e., 0.028 mol X/100 g SAN), is diluted by neat SAN (20 wt % SAN−X), whereas EP-*g*-MA is diluted by neat EPDM (50 wt % EP-*g*-MA). The general SAN/rubber weight composition is systematically 75/25. The effect of the intrinsic reactivity of the SAN reactive groups, i.e., primary amine or carbamate, has been studied in close relation to the phase morphology development. For this purpose, the phase morphology has been analyzed within the range of 1−17 min of mixing time.

2. Experimental Section

2.1. Materials. SAN used in this work was the RONFALIN 2770 from DSM containing 26.5 wt % acrylonitrile ($\bar{M}_n$: 6×10^4). The maleic anhydride grafted rubber (EP-*g*-MA), EXXELOR VA 1801 from EXXON, contained 0.6 wt % or 6×10^{-3} mol/wt % succinic/maleic anhydride groups. The nonreactive rubber was the EPDM, KELTAN 4778, from DSM. Terpolymerization of styrene (55 mol %), acrylonitrile (43 mol %), and a carbamate containing comonomer, {1-methyl-1-[3-(1-methylethenyl)-phenyl]ethyl}carbamic acid 1,1-dimethylethyl ester (2 mol %, see Scheme 2), was initiated by AIBN in toluene at 60 °C for 24 h. It was recovered by precipitation in methanol and characterized by NMR and FTIR. The carbamate pendant groups of functional SAN were derivatized into amines either in solution prior to blending[11] or in situ during the melt blending process.[12] The actual carbamate content was 0.028 mol/wt % or 2 mol %, and the molecular weight was 10^5 with a polydispersity index of 1.5.

2.2. Mixing Conditions. Samples (20 g) were melt blended with a laboratory two-roll mill at 200 °C. A master batch of 50 wt % EPDM and EP-*g*-MA was previously melt blended for 7 min under moderate shearing (rolls speed = 15 and 25 rpm) and stabilized by 0.5 wt % IRGANOX 1010 from CIBA GEIGY. After mixing, the rubbery blend was cooled to room temperature and cut into small pieces (2×5 mm). 20 wt % reactive SAN was then melt blended with neat SAN at 200 °C, followed by the addition of the required amount of the (EPDM/EP-*g*-MA) premixture. One minute later, the shear rate was regularly increased (rolls speed of 0.5 and 25 rpm). The mixing conditions were then maintained. After the specified mixing time, small pieces of blend were sampled out from the mixer and immediately dropped into a liquid nitrogen bath in order to freeze in the phase morphology. Mixing times were 1, 2, 3, 5, 8, 12, and 17 min, respectively. The zero time was the start of feeding of the rubber pellets.

2.3. Transmission Electron Microscopy. Observations were carried out with the transmission electron microscope PHILIPS M100 at an accelerating voltage of 100 kV. Thin sections (90 nm) were prepared by ultramicrotomy (ULTRACUT E from REICHERT-JUNG) at −130 °C and stained by exposure to RuO_4 vapors for ca. 2 h. SAN was observed as darker phases as result of a higher affinity for ruthenium tetroxide compared to EPR. Micrographs were analyzed by using the KS 100 (Kontron Imaging System) software. An average number of 300 particles were considered per sample. The cross-sectional surface area of these particles was converted to an equivalent diameter by eq 1:

$$d_{\text{equivalent}} = (4/\pi(\text{area}))^{0.5} \tag{1}$$

2.4. Interfacial Grafting Conversion. The extent of the interfacial grafting was quantified by a solvent extraction technique. Samples of pelletized blends (1.0 g) were extracted in a Soxhlet apparatus by refluxing acetone, which is a selective solvent for SAN, up to constant weight, i.e., for at least 100 h. The insoluble material was recovered and dried up in a vacuum oven. The soluble fraction was concentrated and precipitated into methanol. The insoluble material was compression molded into films (at 200 °C for 1 min) and quantitatively analyzed by FTIR in order to estimate the amount of SAN-*g*-EP copolymer formed during blend processing, since the content of EP of the extracted SAN appeared to be negligible. Thus, the unreacted SAN was separated from the insoluble mixture of EP-*g*-SAN graft and possibly crosslinked copolymer, unreacted EP-*g*-MA and EPDM. The absorbance, A, of a given constituent of a mixture is related to its concentration, C, according to Beer's law:

$$A = \log I_0/I = abC \tag{2}$$

where b is the thickness of the absorbing medium and a is the molar extinction coefficient. This relationship between A and C may be exploited to gain information about the blend composition, provided that a calibration curve is available. For this, a calibration curve was set up from solvent cast SAN/(EPDM/EP-*g*-MA 1/1) of various molar compositions, hot toluene being the solvent. Variation in film thickness was compensated for by normalizing the SAN absorption at 1492 cm^{-1} (A_{SAN}) with respect to the characteristic EPR absorption at 720 cm^{-1} (A_{EPR}). Because of partial overlap with adjacent peaks, the height of the absorption peaks at 1492 and 720 cm^{-1} was used for calibration and analysis. In the composition range of interest, these "peaks" were of comparable intensity. This calibration curve was fitted by linear regression, in agreement with the following equation:

$$A_{SAN}/A_{EPR} = 0.15953 + 2.0971 C_{SAN}/C_{EPR} \tag{3}$$

The regression coefficient R^2 was 0.99. The nonzero absorbance ratio in the absence of SAN is a consequence of the aforementioned partial overlap of absorption peaks. The fitting parameters were subsequently used along with the A_{SAN}/A_{EPR} ratio measured from the FTIR spectra of the insoluble material to calculate the weight fraction of SAN grafted to the rubbery phase. It must be noted that the grafting efficiency calculated by IR for blends prepared in the melt was in good agreement with the data collected by ESCA for bilayer assemblies (static conditions).[10]

2.5. Charpy Impact Resistance Measurements. Impact tests specimens were machined from the sheets molded at 200 °C for 6 min. This inavoidable thermal posttreatment can however alter the phase morphology although in direct relation to the stability imparted by the "in situ" formed copolymer. This effect (if any) is expected to increase the difference in the impact resistance of the blends prepared from SAN−NH_2 and SAN-carb, respectively. The samples were stored for analysis at room temperature. The Charpy impact strength was then measured at room temperature with a CEAST Fractoscope using ASTM D256B notched specimens (0.35 mm notch).

3. Results and Discussion

3.1. Phase Morphology Development. The dependence of the number-average diameter, D_n, on the mixing time for (SAN/SAN-X)/(EPDM/EP-*g*-MA) (60/15)/(12.5/12.5) is illustrated in Figure 1. D_n data for the blend containing unreactive SAN (no SAN−X) remained essentially unchanged for mixing times longer at the time greater than 8 min and are not reported in the figure. Whatever the blend composition, D_n was measured at mixing times longer than 2 min, i.e., when the rubber was completely melted. The experimental curve is clearly shifted toward smaller particles sizes, when SAN−X compatibilizer (i.e., SAN−NH_2 or SAN−carb)

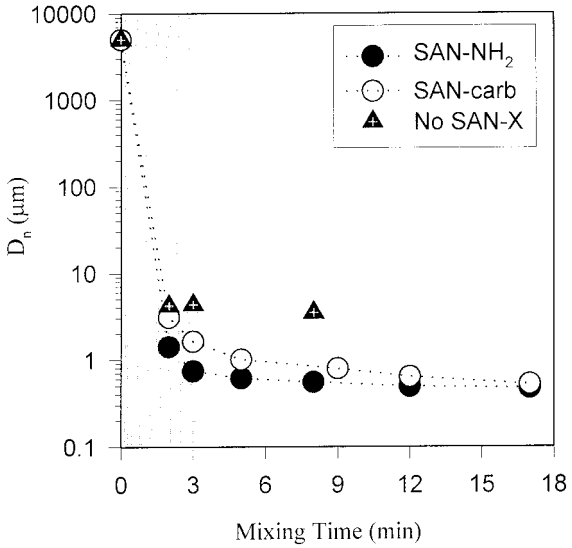

Figure 1. Number-average rubber particle diameter, D_n, vs mixing time for blends modified or not by either SAN−NH_2 or SAN−carb.

is used. This is an indication of the interfacial activity of the in situ formed SAN-*g*-EP graft copolymer. Moreover, the rubber dispersion appears to be more rapidly improved in the case of primary amine containing SAN compared to SAN−carb. However, whatever the type of reactive SAN, the major reduction in the dispersed phase size is observed at short processing times, i.e., during the initial phase of softening and melting of the rubber component (see hatched region in Figure 1). For example, the number-average particle diameter is reduced from ca. 5 mm (rubber pellet size) down to 1 μm within 150 and 300 s mixing in the case of SAN−NH_2 and SAN−carb, respectively.

Longer mixing times affect the phase morphology in a way that however depends on the type of SAN reactive groups. The log-normal distribution plots of Figure 2 illustrates clearly the effect of the SAN reactive groups on the phase morphology for long mixing times, i.e., 5 and 17 min mixing times. In the case of SAN−NH_2 and 5 min blending, the phase morphology consists of a large number of small dispersed particles, along with a small number of larger particles (0.7−2 μm). The major effect of increased mixing time is a reduction in the size of the largest particles, while the smallest rubber domains remain unchanged. This observation confirms that most rubber particles have reached the equilibrium size after 5 min. Consistently, only small changes in both the number-average diameter, D_n, and the volume average diameter, D_v, after 5 min mixing time are observed (Figure 3). In the case of SAN bearing carbamate groups, the phase morphology is developed in a completely different manner within the same period of mixing time (5−17 min). Figure 2 shows that after 5 min mixing substitution of SAN−carb for SAN−NH_2 results in the increase of the average size of the dispersed phases and the broadening of the size distribution. Upon increasing mixing times, the rubber particle size distribution is clearly extended toward smaller values (Figure 2), while at the same time very large and highly deformed rubber domains in a small number are formed. (These particules are not shown in Figure 2 but clearly observed in TEM pictures and taken into account in the average diameter calculation.) The TEM pictures reveal that these large rubber particles

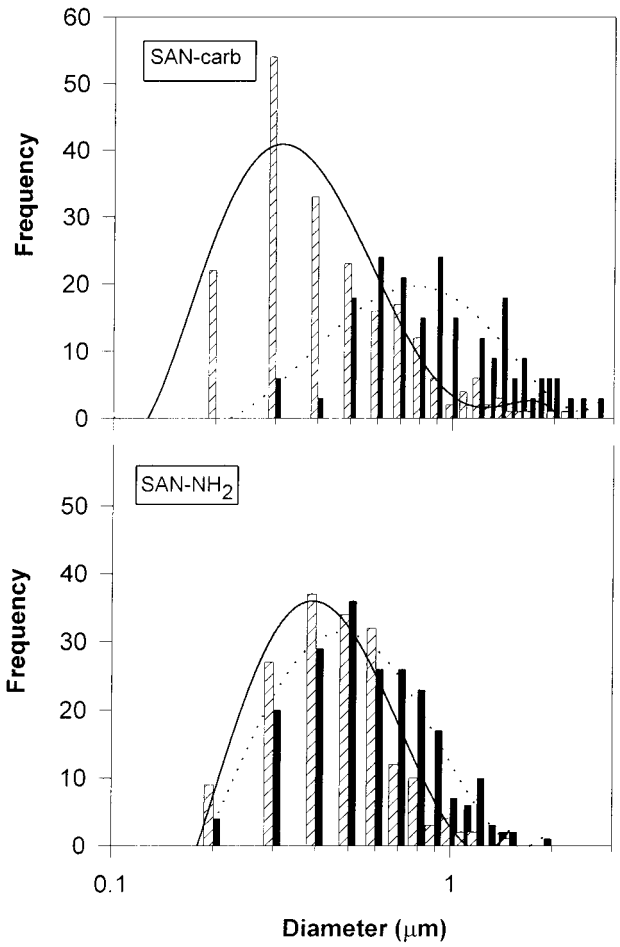

Figure 2. Particle size distribution for blends modified by either SAN−NH_2 or SAN−carb after 5 (- - -, ■) and 17 min (—, ⧄) of mixing.

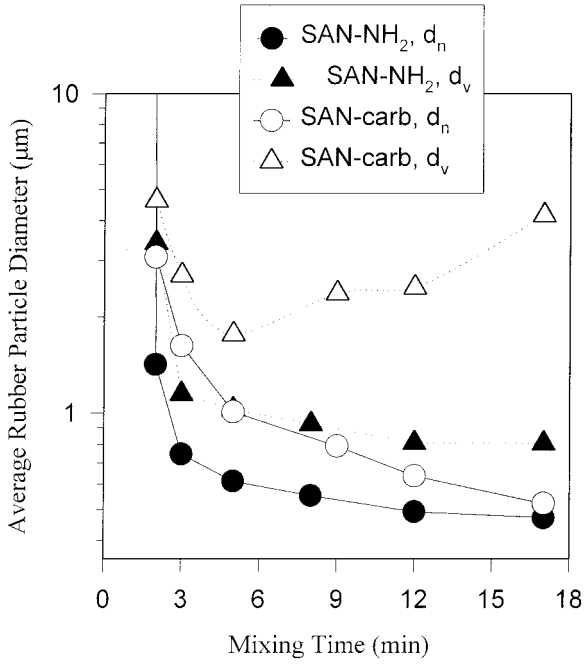

Figure 3. Number- and volume-average rubber particle diameter, D_n and D_v, respectively, vs mixing time for blends modified or not by either SAN−NH_2 or SAN−carb.

are of a composite-type morphology, i.e., containing occluded SAN subphases. As a result, the increasing formation of smaller particles (through a breakup

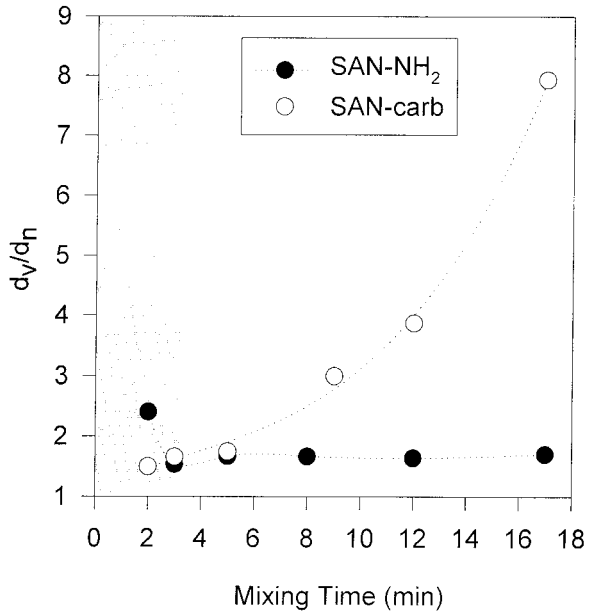

Figure 4. D_v/D_n vs mixing time for blends modified by either SAN−NH_2 or SAN−carb.

mechanism) leads to a significant decrease of D_n with mixing time (Figure 3). But in opposite way, the generation of few very large rubber particles (through coalescence phenomena) can account for the observed increase of D_v as the mixing continues (Figure 3).

The breadth of the particle size distribution may be approximated by the D_v/D_n ratio of the volume average diameter to the number-average diameter. Figure 4 shows the dependence of D_v/D_n on the mixing time. Beyond the softening/melting step, during which the main change in phase morphology is observed (thus after 3 min mixing), D_v/D_n is basically constant in the case of SAN−NH_2, in contrast to the substantial broadening of the particle size distribution when SAN−carb is concerned.

Consistent with the higher reactivity of primary amine toward maleic anhydride compared to the carbamate counterpart, the rubber dispersion occurs more slowly when SAN−carbamate is used rather than SAN−NH_2 and becomes challenged by coalescence phenomena, which leads to the stabilization of large and highly deformed rubber domains of a composite-type morphology, i.e., containing occluded SAN subphases. Clearly, coalescence dominates the mixing process when carbamate groups are attached to SAN, indicating a poor stabilization of the interface as result of a slow interfacial reaction and thus the slow formation of the compatibilizer.[13,14] To support this explanation, the efficiency of SAN−NH_2 and SAN−carb in stabilizing the phase morphology has been compared after 17 min mixing. For this purpose, samples have been compression molded at 200 °C for 30 min and the phase morphology observed by TEM. Table 1 shows that the number-average diameter of the rubber particles is not affected by the 30 min annealing when SAN−NH_2 is used, although D_n is increased by ca. 35% in the case of SAN−carb. So, SAN−NH_2 is much more efficient than SAN−carb to inhibit coalescence and to impart stability to the phase morphology more likely due to the rapid coverage of the interface by a graft copolymer. The decrease in D_v observed whatever the reactive group attached to SAN is thought to be an artifact. Indeed, the bigger the rubber particles are, and the more deformed they are upon compression molding, which can result in smaller apparent D_v calculated from image analysis.

Table 1. Average Diameter of the Dispersed Rubber Phase in Quaternary (SAN/SAN-X 4/1 wt/wt)/(EPDM/EP-*g*-MA 1/1 wt/wt) 75/25 wt/wt Polyblends vs Mixing Time (min)

mixing time	SAN−NH_2			SAN−carb		
	D_n (μm)	D_v (μm)	D_v/D_n	D_n (μm)	D_v (μm)	D_v/D_n
2	1.42	3.40	2.4	3.08	4.62	1.5
3	0.75	1.15	1.55	1.62	2.7	1.65
5	0.61	1.03	1.65	1.01	1.76	1.75
8	0.55	0.92	1.65	0.79	2.37	3
12	0.49	0.81	1.65	0.64	2.47	4
17	0.47	0.80	1.7	0.52	4.15	8
17 + 30[a]	0.49	0.69	1.4	0.70	3.95	6

[a] These samples were compression molded at 200 °C for 30 min.

3.2. Composite EPR Droplets. Transmission electron micrographs show that the dispersed rubber domains contain SAN subinclusions of an average diameter in the range from 0.5 μm to less than 50 nm. As a rule, the relative amount of SAN subinclusions increases with the mixing time and when SAN−carb is used rather than SAN−NH_2. It must be noted that only few SAN subinclusions are formed in the rubber phase in the case of nonreactive blending. Therefore, rate and completeness of the grafting reaction appear to have a decisive role in the subinclusions' formation. This qualitative analysis has been completed by the image analysis of the dispersed phases. The cross-sectional surface area of the dispersed phases (S_f) and the SAN subinclusions (S_{sub}) has indeed been measured, from which the surface area occupied by the rubber (S) has been inferred (eq 4):

$$S = S_f - S_{sub} \tag{4}$$

Figure 5b shows a straight line of slope 1, which confirms the absence of subinclusions, in the case of SAN−NH_2, i.e., independent of the mixing time and the particle size. At constant S value, substitution of carbamate groups for amines results in S_f, as larger as both the size of the dispersed phase and the mixing time are increased, which is the evidence of steadily more important subinclusions (Figure 5a). According to Favis et al.,[15] the volume ratio of subinclusions with respect to the dispersed phase (sub. %) may be approximated by the area ratio calculated from the image analysis of TEM micrographs, in agreement with eq 5:

$$\text{sub. (\%)} = [(S_f - S)/S_f] \times 100 \tag{5}$$

When polyblends contain SAN−carb, the relative amount of occluded SAN is in the range from from 1.5 to 17.17%, depending on both the mixing time and the rubber particle size, whereas almost no SAN subinclusions are observed in the case of SAN−NH_2.

It is worth pointing out that Maréchal[13] observed the formation of subinclusions independent of the mixing time in the specific case of a fast NH_2/MAH reaction occurring mostly during the melting/softening step of the polymers blending. As a rule, these subinclusions should result from local phase inversion during the melting step, just before the phase morphology is stabilized.[14] In the case of the slow carbamate/MAH interfacial reaction, the formation of subinclusions is

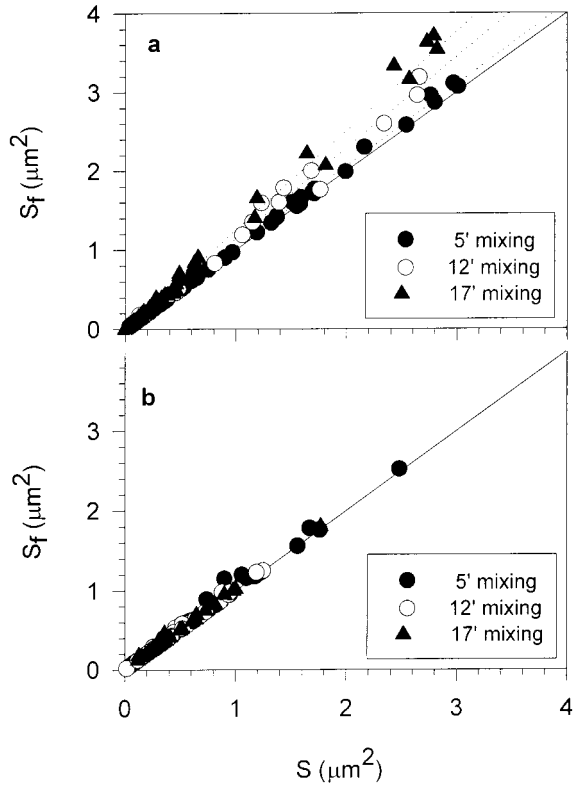

Figure 5. Total surface area of the dispersed phase (S_f) vs surface area of the dispersed rubber component (S). $S_{sub} = S_f - S$ is the surface area of the SAN subinclusions in the dispersed phases. Data have been plotted for polyblends modified by either (a) SAN−carb or (b) SAN−NH_2 and different mixing times, i.e., 5, 12, and 17 min.

thought to result from phase coalescence that challenges dispersive mixing as long as the coverage of the interface by graft copolymer is not high enough. This may explain why the subinclusion formation increases with the mixing time, in contrast to what happens when the fastly reacting SAN−NH_2 is used. Moreover, formation of subinclusions decreases the amount of copolymer available at the interface between the SAN matrix and the rubber particles, because part of the graft copolymer is now trapped in the rubber phases (at the rubber/subinclusions interface). Although of larger size, the rubber particles that contains subinclusions (1−2 μm^2) with copolymer at their surface appear to resist efficiently the breakup (Figure 6b), which contributes to account for data reported in Figure 5a.

3.3. Grafting Rate. To estimate the yield of the grafting reaction, unreacted SAN has been extracted by refluxing acetone. The percentage of SAN grafted to the rubber phase has been calculated from the FTIR spectrum of the insoluble material.

Figure 7 compares the FTIR spectra of the (SAN/SAN−NH_2)/(EPDM/EP-*g*-MA) extracted polyblends at 1, 5, and 17 min mixing, together with the spectra of the SAN and rubber components. Peaks characteristic of the rubber phase (720 cm^{-1}) and the SAN phase (1601, F: 1492 and A: 2236 cm^{-1}) show that the relative intensity of the SAN absorption (e.g., absorptions A and F; Table 2) with respect to that of an internal absorption reference (EPR: at 720 cm^{-1}) increases with mixing time, whereas the small stretching vibration of the anhydride carbonyl at 1789 cm^{-1} (Table 2: absorption B) decreases simultaneously. The interfacial grafting reaction product shows up new absorptions in the 1650−1750 cm^{-1} region (absorptions D and E) and at 1220 cm^{-1} (absorption G).

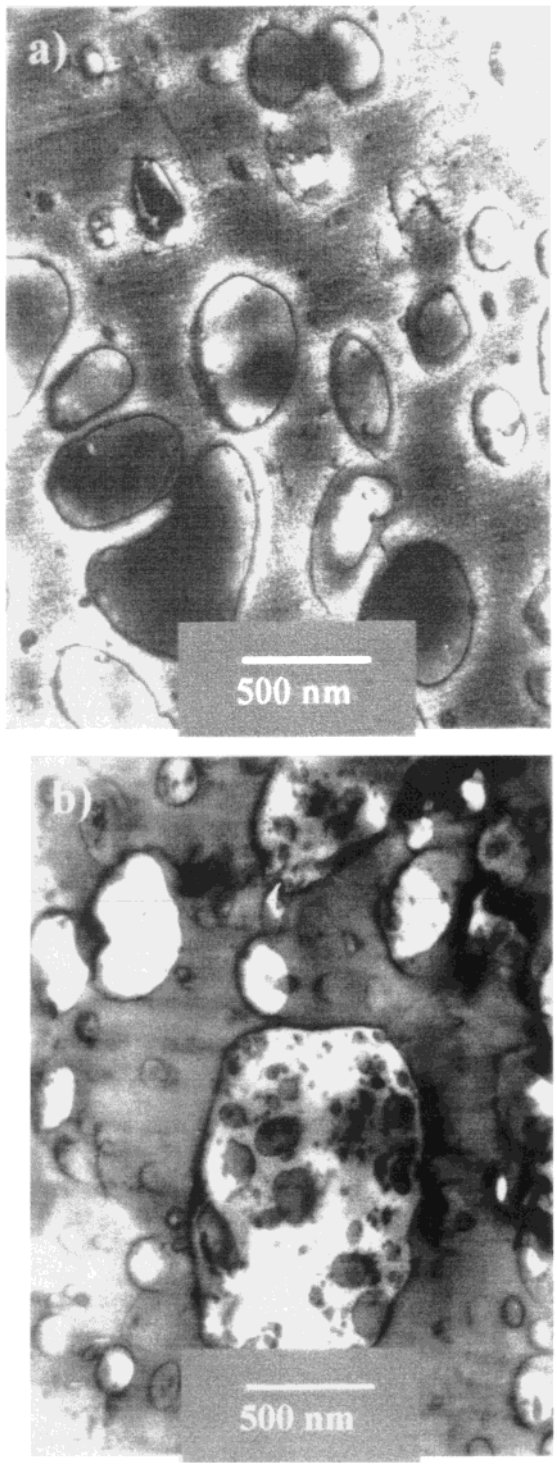

Figure 6. TEM micrographs for the 75/25 wt/wt quaternary blends of (a) (SAN/SAN−carb 4/1 wt/wt) and (EPDM/EP-*g*-MA 1/1 wt/wt) and (b) (SAN/SAN−NH_2 4/1 wt/wt) and (EPDM/EP-*g*-MA 1/1 wt/wt) after 17 min mixing.

The reaction of amine and anhydride attached to polymers has been studied elsewhere. For instance, Song et al.[16] concluded the formation of amide or imide bonds. The reactions were carried out in a roller blades mixer at 180 °C and 100 rpm rotor speed for 20 min. Bourland et al.[17] reported that anhydride of SMA reacted instantaneously to form amidic acid in solution at ambient temperature. Imide ring closure was ob-

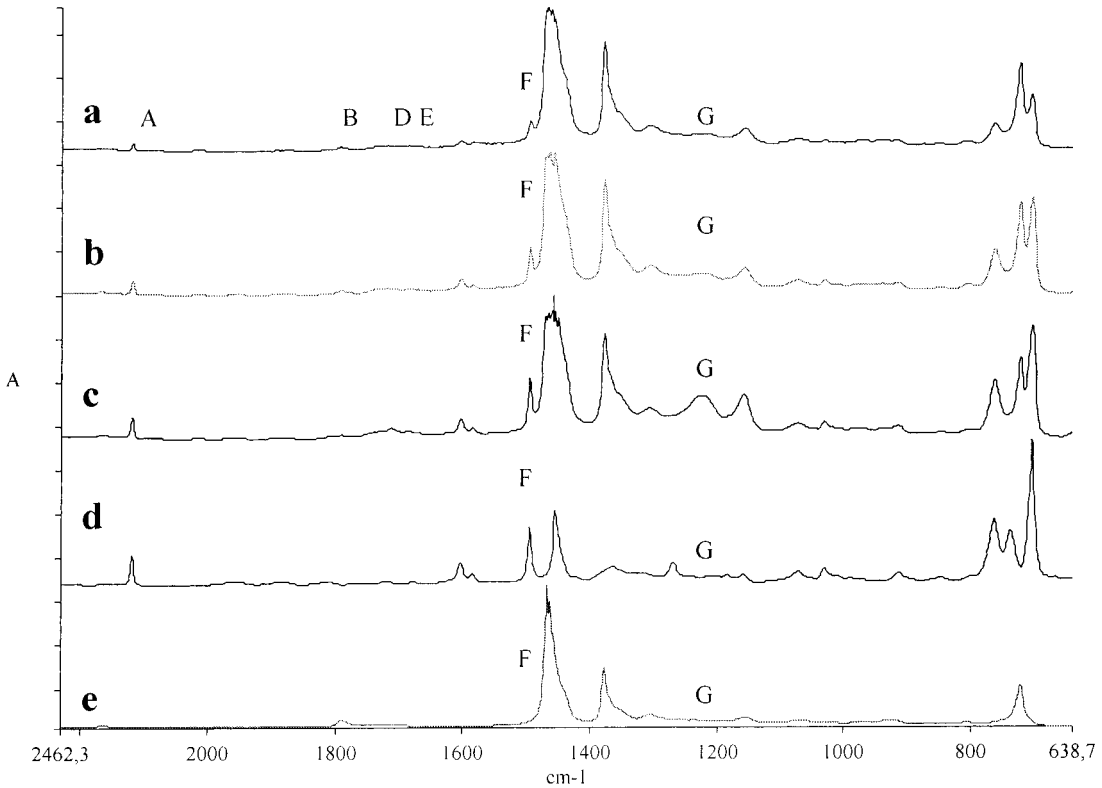

Figure 7. Infrared spectra (absorbance) of the extracted 75/25 wt/wt quaternary blends of (SAN/SAN−NH_2 4/1 wt/wt) and (EPDM/EP-*g*-MA 1/1) after (a) 1, (b) 5, and (c) 17 min mixing and of (d) SAN−NH_2 (0.028 mol NH_2/wt %) and (e) (EPDM/EP-*g*-MA 1/1 wt/wt) preblend. See also Table 2.

Table 2. Relative Intensity of the Absorption Bands Involved in the SAN−NH_2/EP-*g*-MA Interfacial Reaction (Internal Absorption Reference at 720 cm^{-1})

	absorption bands (cm^{-1})						
	A 2235 nitrile	B 1789 anhyd	C 1770 imide	D 1700 acid/imide	E 1680 amide	F 1492 styrene	G 1220 acid/amide
rubber[a]		0.1					
SAN[b]	inf					inf	
1 min	0.06	0.06		0.07	0.05	0.26	0.20
5 min	0.18	0.05		0.08	0.07	0.53	0.24
17 min	0.30	<0.04		0.13	0.09	0.75	0.52

[a] Rubber stands for the (EPDM/EP-*g*-MA 1/1) mixture. [b] SAN stands for SAN−NH_2 (0.028 mol NH_2/wt %).

served to occur in solution-cast films at elevated temperatures (220 °C) and was the rate-determining step.

There is no clear indication that imide is formed in the occasion of the grafting reaction carried out at 200 °C. Indeed, the new absorption observed at 1220 cm^{-1} (absorption G) is not characteristic of the imide but rather of the acid/amide moiety. The absorption of the imide at 1770 cm^{-1} (asymmetrical stretching) is not observed, whereas the 1720−1700 cm^{-1} characteristic symmetrical stretching[18,19] cannot be discriminated from the absorption of the carbonyl stretching of the carboxylic acid[16] at ca. 1700 cm^{-1}. In this study, the steric hindrance of the primary amine (two methyl groups on the α-carbon, Scheme 2) could explain that acid/amide cyclization into imide is a difficult reaction. The use of SAN−carb instead of SAN−NH_2 leads to quite comparable infrared spectra, except for additional carbonyl absorption of the carbamate at 1717 cm^{-1}.

Figure 8 shows the mixing time dependence of the conversion of SAN−NH_2 and SAN−carb into grafted copolymer. It is clear that the kinetics of the grafting reaction strongly depends on the intrinsic reactivity of the functional SAN groups toward maleic anhydride. In the case of primary amine bearing SAN, the reaction is quite fast, since ca. 25% conversion has occurred for the 3 first min of mixing, i.e., for the time required by the softening and melting of the rubber pellets (hatched region in Figure 8). During the next mixing step, the grafting conversion is much slower (additional 20% conversion for 15 min mixing) more likely as a result of the interface occupation by the already formed copolymer and the related phase stabilization.[10] In contrast to SAN−NH_2, the grafting of SAN−carb is very limited during the softening and melting step of the blend components, indicating a lower apparent reactivity of SAN−carb compared to that of SAN−NH_2.

Actually, the rate constant of the carbamate thermolysis into primary amine has been determined from TGA measurements of a SAN−carb sample containing 0.049 mol carb/wt %. Preliminary, TGA experiments were conducted from 20 to 600 °C at a heating rate of 10 °C/min, under air. A transition was observed between 200 and 250 °C, which was assigned to the thermolysis of the carbamate moieties into primary amines with release of carbon dioxide and isobutene. A good agreement was found between the announced carbamate

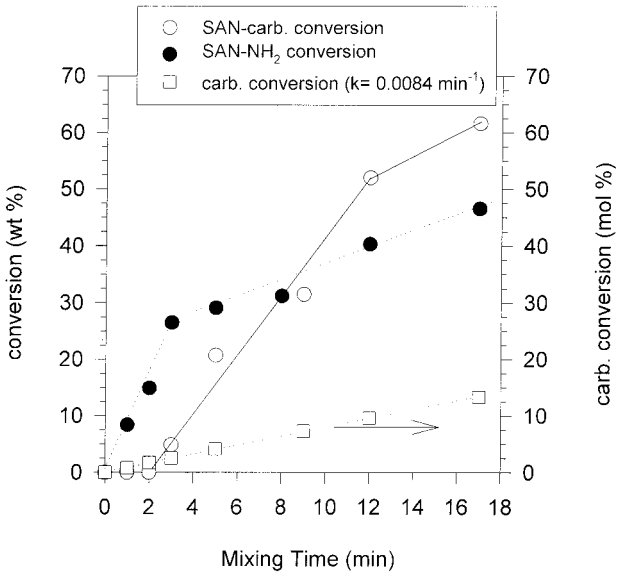

Figure 8. SAN−X conversion (as estimated from extracted samples, see experimental part) vs mixing time for polyblends modified by either SAN−carb or SAN−NH_2.

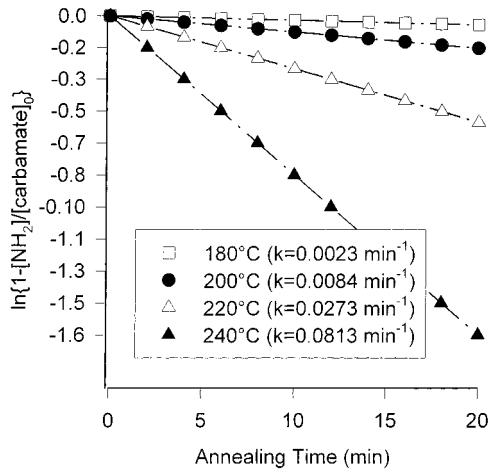

Figure 9. Fraction of carbamate groups converted into primary amines ($[NH_2]/[carbamate]_0$) vs time at various temperature, i.e., 180, 200, 220, and 240 °C.

content of reactive SAN, i.e., 0.049 mol/wt %, and the value estimated from the experimental weight loss in the 200−250 °C range. The conversion of carbamate groups into free amines was then measured by TGA of the SAN−carb under isothermal treatment at various temperatures, i.e., 180, 200, 220, and 240 °C (Figure 9). The thermolysis reaction was found to be first order with respect to carbamate, and an activation energy of 115 kJ/mol was calculated (Figure 10). At the usual mixing temperature of 200 °C, the rate constant of the carbamate thermolysis was found to be 0.0084 min^{-1}.

The carbamate decomposition into amine is thus very slow, since it does not exceed 4 and 13 mol % after 5 and 17 min mixing, respectively (Figure 8). This carbamate decomposition is the rate-determining step of the grafting reaction. Beyond the melting of the constitutive polymers, the grafting yield increases much more rapidly in the case of SAN−carb compared to SAN−NH_2, although the concentration of the amine released by the carbamate thermolysis is lower. When the mixing time exceeds 9 min, the higher grafting efficiency is observed for the less apparently reactive SAN−carb.

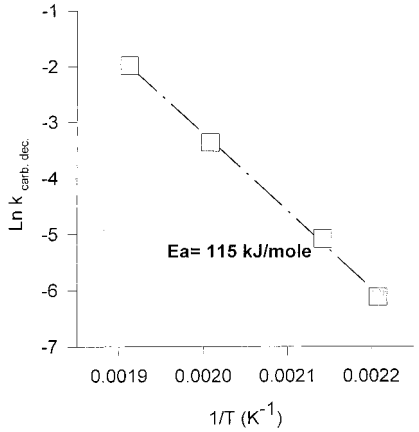

Figure 10. Arrhenius plot for the carbamate thermolysis.

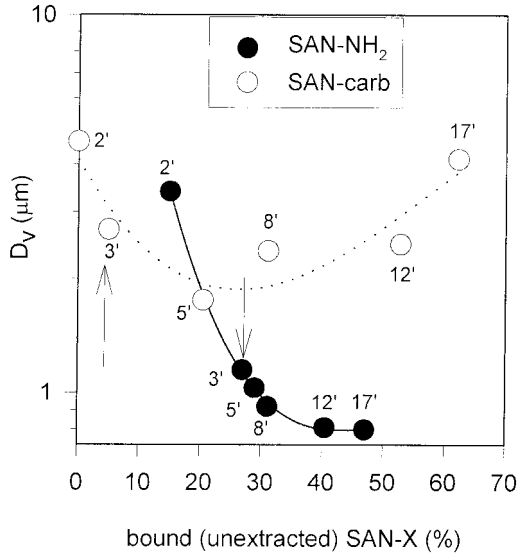

Figure 11. Volume-average rubber particle diameter, D_v, vs SAN−X conversion for polyblends modified by either SAN−carb or SAN−NH_2.

The only way to explain this unexpected result is to consider the subinclusions, which are a source of error in the calculation of the amount of grafted SAN (based on SAN extraction). So, the calculated values must be considered as lower limit values, particularly in the case of SAN−carb. Indeed, in the case of SAN−carb, increasing the mixing time results in an increased probability of interfacial grafting and compatibilizer formation, but a part of it (with probably neat SAN) will be trapped as subinclusions. Bound SAN−carb molecules are then partitioned between the EPR/SAN matrix interface and the EPR phase, respectively. Compared to SAN−carb, at constant conversions, the highly reactive SAN−NH_2 is more preferentially grafted at the proper interface, i.e., between the SAN matrix and the EPR domains, and more effective in emulsifying the rubber dispersion. An indirect confirmation of this hypothesis may be found in Figure 11, in which the volume average particle diameter has been plotted as a function of the amount of bound (unextracted) SAN. In the case of SAN−NH_2, D_v decreases regularly with the fraction of reacted SAN. This behavior can be seen as an indirect proof of the localization of bound SAN at the proper interface, i.e., between the SAN matrix and the EPR dispersed phase. In contrast, in the case of SAN−carb and beyond 5 min mixing (i.e., in the melt state), D_v increases continuously

although an increased amount of SAN has been grafted on the rubber. We can assume that at the same time an increasing fraction of this bound SAN becomes occluded within the rubber domains and cannot play its interfacial activity in stabilizing rubber particles, which then coalesce. This mechanism is consistent with (i) the increasing formation of SAN subinclusions with the blending time and (ii) the quasi-absence of theses subphases in the case of nonreactive blends. Although the extraction of the unreacted SAN subincluded in the rubber phase has been considered, only partial solubility of the rubber in hot toluene (an usual solvent of it) has prevented reliable data from being collected. The interfacial reaction between multifunctional SAN and EP-*g*-MA could account for this problem.

The efficiency of any compatibilizer in improving the phase dispersion is reflected by the average area (A) it occupies at the interface.[20−24] Within the limits of the assumption that all the compatibilizer molecules are and remain at the interface, Paul and Newman[25] proposed to express A by eq 6:

$$A = S_{sp}M/(N_{av}W) \tag{6}$$

with

$$S_{sp} = (6/D_n)\Phi_d \tag{7}$$

where S_{sp} is the blend specific interfacial area, M is the number-average molecular weight of the compatibilizer, W is its wt/vol content, N_{av} is the Avogadro number, D_n and Φ_d are the number-average diameter and the volume fraction of the dispersed rubber phase, respectively. In this study, M and W are unknown since graft copolymer cannot be isolated and characterized. As a rough approximation, the reactive SAN and the amount of grafted SAN have been used in eq 7. M and W are thus underestimated, this error being compensated by the fact that A depends on the ratio of these parameters.

Since the validity of eq 6 is based on the assumption that all bound SAN chains are at the interface between the matrix and the dispersed phase, the calculation of cross-sectional surface area per grafted SAN chain (A) has been performed only in the case of SAN−NH_2. Beyond the melting and softening of the constitutive components, i.e., after 3 min mixing, this interfacial area does change significantly with the mixing time (10 ± 1 nm^2). So, in the case of primary amine, the system reaches rapidly a constant interfacial copolymer concentration (i.e., $1/A$), such that the interface coverage by grafted SAN chains is maximum and effective in inhibiting coalescence. This situation should suggest that the NH_2/MAH reaction ($\Delta SAN_{bound}/\Delta t$) is fast enough to cover the interface as fast as it is generated ($\Delta S_{sp}/\Delta t$), since $(S_{sp}/SAN_{bound})_t$ (which is related to A, see eq 6) is basically independent of the mixing time (t). Similar conclusions were drawn by Orr et al.[10] in the case of anhydride terminal PI/aliphatic amine terminal PS blends. The rate of interfacial area generation controls the evolution of grafting reaction.

Although the calculation of A is not possible in the case of SAN−carb (a significant part of reacted SAN being occluded), we can expect that the interface is covered by graft copolymer much more slowly, since SAN−carb is less reactive compared to SAN−NH_2. This slower interface covering allows the phase dispersion (or interface generation) to be challenged by phase coalescence. The final morphology thus strongly depends on the rate at which the phase morphology is developed compared to the copolymer formation.

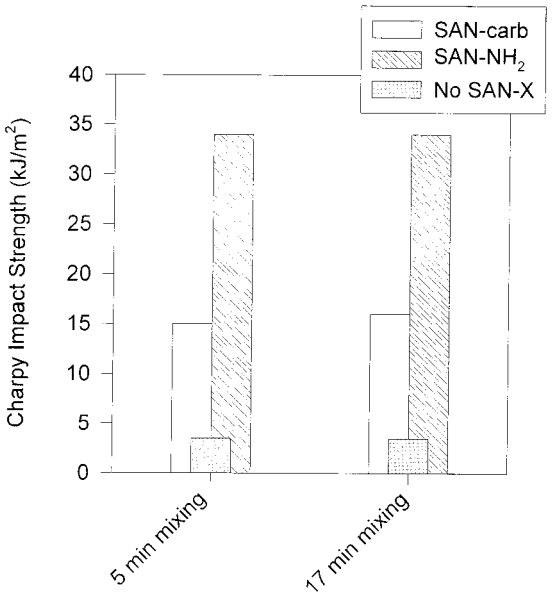

Figure 12. Charpy impact resistance for blends modified by either SAN−NH_2 or SAN−carb after 5 and 17 min of mixing.

3.4. Charpy Impact Properties. In Figure 12 is plotted the Charpy impact strength for polyblends modified by either SAN−NH_2 or SAN−carb after 5 and 17 min mixing, respectively. For the sake of comparison, the impact properties of nonreactive blends, which contain no reactive SAN, are also given. Consistent with the higher reactivity toward maleic anhydride, SAN−NH_2 is more efficient than SAN−carb in order to provide polyblends with high toughness. For instance, the SAN−carb modified polyblends (15−16 kJ/m^2) never achieve the ductility of SAN−NH_2 containing blends (34 kJ/m^2). On the other hand, whatever the type of SAN reactive groups, the impact strength is basically independent of the mixing time.

In the case of primary amine, after 5 min mixing, the interface coverage by grafted chains is high enough to impart high interfacial adhesion to the polyblends, such that subsequent mixing does not result in an impact improvement. This observation is also consistent with the known dependence of the impact resistance on the rubber particle size 1 and the fact that most rubber particles reached their final size after ca. 5 min of mixing.

In the case of SAN−carb, the mixing time influences the amount of the in situ formed compatibilizer, and it affects its localization. As mixing continues, an increasing fraction of copolymer stabilizes the interface between the rubber and the subinclusions concurrently with the grafting at the SAN matrix/rubber interface. Thus, when grafting is challenged by coalescence (this is the case of SAN−carb), increasing the mixing time leads to the increasing formation of copolymer, but not localized at the proper interface. These results underline the beneficial effect of grafting during melting and softening, i.e., before coalescence takes place (this is the case of SAN−NH_2) in order to generate the compatibilizer where it is needed. The difference in the average size of the rubber particles, depending on the reactive groups attached to SAN, may also contribute to the observations reported in Figure 12. This issue will be discussed in more detail in a forthcoming paper.

3.5. Dispersion Mechanism. At the very early stage of mixing, i.e., when the rubber pellets are added in the molten SAN, the abrasive forces are very high, improving rapidly the rubber dispersion. During this step, the interfacial area is continuously increasing, making additional sites available to grafting, and vice versa, the interfacial reaction is expected to decrease the interfacial tension and thus to favor a larger interfacial area. Since the primary amine−maleic anhydride reaction is fast enough to cover the interface as fast as it is generated, copolymer is rapidly formed in an amount large enough to stabilize this interface, when SAN−NH_2 is processed. When the softening/melting is over, both particle size and progress of the interfacial reaction seem to level off or at least to improve much less rapidly, as result of an efficient protection of the interface toward additional reactive chains. The next dispersive mixing is therefore poorly efficient, so that most rubber particles have reached final size after ca. 5 min mixing.

When the protected amines are attached to SAN, the interfacial grafting reaction is controlled by the slow thermolysis of carbamate groups into amines, which explains why it essentially occurs beyond the softening/melting step of all components, and likely slower than the interface area generation. During the next dispersive mixing step, a competition between phase dispersion and phase coalescence takes place. This competition will fall under control of the progress of the interfacial reaction, which progressively reduces the interfacial tension, makes the particle breakup easier, and stabilizes the interface against coalescence. As proposed by De Roover,[6] the phase coalescence essentially takes place when the blended components are completely melted because then the shear forces are weaker compared to the situation in which solid and melted phases coexist. On the occasion of coalescence of poorly stabilized rubber phases, graft copolymer originally at the rubber/SAN matrix interface may be occluded together with neat SAN within larger rubber phases, which are to some extent stabilized against breakup. Then, the dispersion/coalescence competition can account for the broadening of the particle size distribution reported in Figures 3 and 4.

4. Conclusions

In agreement with observations reported by several authors,[3−6,8] the main changes in phase occur during the first few minutes of mixing, i.e., when the blend components are softening and melting.

Since the primary amine−maleic anhydride reaction is fast enough to cover the interface as fast as it is generated, it mainly occurs during the initial dispersion step, when SAN−NH_2 is processed. This explains why most rubber domains attain a nearly constant size after 5 min mixing. The rubber particles are then stabilized to the point where neither phase coalescence nor phase breakup has a significant effect during subsequent mixing.

In the case of SAN bearing carbamate groups, the interfacial reaction is controlled by the (slow) carbamate thermolysis into primary amine. Then, compared to SAN−NH_2, the grafting of SAN−carbamate is a much slower reaction, taking place essentially after the softening/melting of the blend components. During the so-called dispersive mixing, phase dispersion is then challenged by coalescence. The rubber phase coalescence is responsible for SAN occlusions leading to the formation of large composite-type dispersed rubber domains. This phase morphology is progressively stabilized as the reaction at the rubber/SAN matrix interface and the rubber/SAN inclusion interface makes progress.

Thus, SAN−NH_2 is more efficient than SAN−carbamate in stabilizing fine rubber particles of a narrow size distribution even for long mixing times. This conclusion emphasizes how important is the rate at which the interfacial grafting reaction occurs with respect to the melting/softening of the blend components and the time required for phase coalescence to become efficient. So, the final morphology strongly depends on the relative kinetics for the phase morphology to develop and the graft copolymer to be formed at the interface.

Acknowledgment. C.P. and R.J. are grateful to the "Services Fédéraux des Affaires Scientifiques, Techniques et Culturelles" for general support in the frame of the "PAI-4: Chimie et Catalyze Supramoléculaire". They also thank Dr. I. Luzinov for stimulating and helpful discussions and Mrs M. Dejeneffe for assistance with cryoultramicrotomy. The authors are much indebted to DSM for financial support and a fellowship to one of them (C.P.).

References and Notes

(1) Van Duin, M.; Koning, C. E.; Pagnoulle, C.; Jérôme R. *Prog. Polym. Sci.* **1998**, *23*, 707.
(2) Xanthos, M. *Polym. Eng. Sci.* **1988**, *28*, 1392.
(3) Scott, C. E.; Macosko, C. W. *Polym. Bull.* **1991**, *26*, 341.
(4) Sundararaj, U.; Macosko, C. W.; Rolando, R. J.; Chan, H. T. *Polym. Eng. Sci.* **1992**, *32*, 1814.
(5) Favis, B. D. *J. Appl. Polym. Sci.* **1990**, *39*, 285.
(6) De Roover, B. Ph.D. Thesis, Université Catholique de Louvain, Belgium, 1994.
(7) Bourry, D.; Favis, B. D. *Polymer* **1998**, *39*, 1851.
(8) Scott, C. E.; Macosko, C. W. *Polymer* **1994**, *35*, 5422.
(9) Orr, C. A.; Adedeji, A.; Hirao, A.; Bates, F. S.; Macosko, C. W. *Macromolecules* **1997**, *30*, 1243.
(10) Pagnoulle, C.; Jérôme, R. *Polyblends' 97 SPE RETEC*, Oct 9−10, 1997, IMI Boucherville, Qc, Canada, Oral Communication. (b) Pagnoulle, C.; Koning, C. E.; Leemans, L.; Jérôme, R. *ACS, PMSE Prepr.* **1998**, *79*, 104. (c) Pagnoulle, C.; Moussaif, N.; Riga, J.; Jérôme, R. *J. Polym. Sci., Part A*, submitted.
(11) Pagnoulle, C.; Koning, C. E.; Leemans, L.; Jérôme, R. Dutch Application No. 1007074, 1997.
(12) England, W. P.; Stoddard, G. J.; Scobbo, J. J. US Patent No. 5310795, 1994.
(13) Maréchal, Ph. Ph.D. Thesis, Université Catholique de Louvain, Belgium, 1993.
(14) Sundararaj, U. Ph.D. Thesis, University of Minnesota, 1994.
(15) Favis, B. D.; Lavallee, C.; Deredouri, A. *J. Mater. Sci.* **1992**, *27*, 4211.
(16) Song, Z.; Baker, E. *J. Polym. Sci., Polym. Chem.* **1992**, *30*, 1589.
(17) Bourland, L. G.; London, M. E.; Cooper, T. A., private communication, 1989.
(18) Sroog, C. E.; Endrey, A. L.; Abramo, S. V.; Berr, C. E.; Edwards, W. M.; Olivier, K. L. *J. Polym. Sci., Part A-1* **1965**, *3*, 1373.
(19) Mathisen, R. J.; Yoo, J. K.; Sung, C. S. P. *Macromolecules* **1987**, *20*, 1414.
(20) Kim, J. K.; Kim, S.; Park, C. E. *Polymer* **1997**, *38*, 2155.
(21) Favis, B. D. *Polymer* **1994**, *35*, 1552.
(22) Tang, T.; Huang, B. *Polymer* **1994**, *35*, 281.
(23) Cigana, P.; Favis, B. D. *Polym. Mater. Sci. Eng.* **1995**, *73*, 16.
(24) Hosada, S.; Kojima, K.; Kanda, Y.; Aoyagi, M. *Polym. Networks Blends* **1991**, *1*, 51.
(25) Paul, D. R.; Newman, S. *Polymer Blends;* Academic Press: New York, 1976; Vol. 2.

MA991314D